Hypervelocity Impact of a Thin Plate on a Semi-Infinite Slab[1]

B. A. SODEK, Jr. and F. C. TODD,

Department of Physics, Oklahoma State University, Stillwater

INTRODUCTION

A computer solution is presented for the impact of a thin aluminum plate, moving at hypervelocity, on a stationary, semi-infinite, aluminum slab. The solution is obtained by the same procedure used in solving for the impact of microparticles at hypervelocity on space vehicles. Hypervelocity is defined as a velocity in excess of the velocity of sound in both of the impacting materials. The numerical values for the curves in this report are for an initial velocity of the thin plate of 36 kilometers per second, or 118,000 feet per second. The results were obtained in a non-dimensional form; and consequently, solutions for other configurations may be obtained from the data. This solution illustrates the velocity distribution at the start of the impact, the generation and the propagation of the shock into the moving thin plate and into the infinitely thick slab, and the amount of compression that is produced by the shock wave.

An estimate of the pressure from the initial kinetic energy, $\frac{1}{2}Pv^2$, for the thin plate indicates that the pressure from the impact is in the multi-megabar range; i.e. from several million to several tens of millions of atmospheres. At these pressures, investigators assume that any material flows as a perfect, non-viscous fluid so that the standard equations of hydrodynamic flow may be employed. (Walsh *et al.*, 1958; Bjork, 1959; Sodek *et al.*, 1963).

HYDRODYNAMIC EQUATIONS

The problem is solved in Eulerian co-ordinates which give the values of the variables at mesh points in ordinary laboratory, or Cartesian co-ordinates. A total of five relations are required to obtain a solution for the propagation to a shock front and these equations are presented in Fig. 1. The first three equations express the conservation of mass, momentum, and energy, respectively. A fourth relation is not given specifically, but it requires that the entropy must increase across the shock front. This condition is satisfied by the introduction of a pseudo-viscosity term, q, which appears in the first three equations and is defined in equation 5. The introduction of this term was suggested by John von Neumann (von Neumann *et al.*, 1950) and made possible a relatively simple solution for the propagation of the shock with a computer. The partial differential in equation 5 is the gradient of the velocity. By multiplying the true velocity gradient by the absolute value of the velocity gradient, the term q always has the sign which opposes either a positive, or a negative, change in the pressure.

The fifth relation, which is given as equation 4, is an equation of state which thermodynamic considerations require to employ three variables; these are the pressure, the density, and the energy density. The equation of state must be valid over the range of these variables in the problem. A suitable relation for aluminum is the Mie-Gruneisen equation of state. It is deduced from experimental data and theoretical considerations. The method of obtaining this equation was described in previous papers in this

[1]Supported by National Aeronautics and Space Administration Contract No. NASr-7 administered through Research Foundation, Oklahoma State University.

Conservation of Mass:

$$\frac{\partial \rho}{\partial t} + \frac{\partial (\rho V)}{\partial x} = 0 \tag{1}$$

Conservation of Momentum:

$$\frac{\partial (\rho V)}{\partial t} + \frac{\partial \{(p+q) + \rho VV\}}{\partial x} = 0 \tag{2}$$

Conservation of Energy:

$$\frac{\partial (\rho E)}{\partial t} + \frac{\partial \{(p+q)V + \rho VE\}}{\partial x} \tag{3}$$

Mie-Gruneisen Equation of State:

$$p - p_H = \alpha\rho (E - E_H) \tag{4}$$

Artificial Dissipation:

$$q = -A_1^2 \rho \frac{\partial V}{\partial x} \left(\left| \frac{\partial V}{\partial x} \right| \right) \tag{5}$$

ρ, density — x, distance

V, material velocity — t, time

E, specific energy — α, Gruneisen Ratio

p, pressure

Fig. 1. Equations of Hydrodynamic Flow

series (Lake, 1962; Sodek, 1963). The Mie-Gruneisen equation gives the pressure as a functon of the density and energy at any point in terms of p_H and E_H on the Hugoniot curve. The value of *alpha*[1] is a known function of the density. The Hugoniot curve is the pressure-density locus of the final states of shock compression. After compression with an increase in entropy, the material expands along an adiabatic curve for the non-viscous material.

The above equations are converted to a non-dimensional form to conserve computer storage and for convenience in scaling numerical magnitudes. From the dimensionless solution, problems with different velocities of impact and different dimensions are readily obtained. In the present case, the thickness of the thin plate determines the time scale for the calculation. To avoid a specific case, results will be given with arbitrary units of distance and time.

The Numerical Method

The partial differential equations are converted to finite difference equations for solution on a computer by methods which are similar to those

[1]Greek letters used in the figures are spelled out in the text.

that were reported by Longley (1960). The method of transformation is illustrated in Fig. 2. The involved region in space is covered with an equally spaced mesh which creates a number of cells. The thin plate moves parallel to the x-axis of the coordinate system. For every solution corresponding to an instant of time, each mesh has a numerical value of the density, velocity, energy, pressure, and viscosity which represents the mean value of the quantity in that cell. These values vary with time. The system of partial differential equations is replaced by a set of ordinary, algebraic, simultaneous, difference equations. This is accomplished by replacing the differentials with small, but finite increments. The pro-

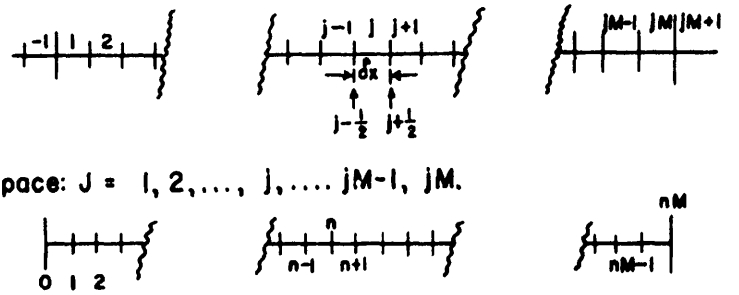

(a) Finite Difference Net.

$$\frac{\partial(\rho V)}{\partial x} \longrightarrow \frac{(\rho V)^{n}_{j+1/2} - (\rho V)^{n}_{j-1/2}}{\Delta x}$$

$$\frac{\partial \rho}{\partial t} \longrightarrow \frac{\rho_j^{n+2} - \rho_j^{n}}{\Delta t}$$

Equation (1) is,

$$\rho_j^{n+1} = \rho_j^{n} + \frac{\Delta t}{\Delta x}\left\{(\rho V)^{n}_{j-1/2} - (\rho V)^{n}_{j-1/2}\right\}$$

(b) Example of Differenced Equation.

Figure 2. Illustration of Finite Difference Method.

cedure corresponds to the use of central differences instead of space derivatives and forward differences in place of time derivatives.

As an example, known values for all parameters in cells at the time, $n\Delta t$, permit the calculation of the density in any cell, j, for the time, $(n+1)\Delta t$ from Equation 1. This is illustrated in Fig. 2. New values for all other parameters may be obtained with suitable difference equations from the original difference equations. The order is to calculate the density, velocity, energy, pressure, and viscosity for the new time. This procedure is repeated for as many times as are desired to carry the solutions for all dependent variables forward in time for each cell in the net. This cyclic procedure was programmed and run on an IBM 650 computer.

RESULTS

From the preceding description of the method for obtaining a solution, it is obvious that the solution must start from an instant when the values of all parameters are known. The initial conditions at the time zero are illustrated in Fig. 3. Initially, the thin plate is fifteen units in length and placed immediately adjacent to the semi-infinite target. Both projectile and target are aluminum. The initial velocity of every point in the thin plate is the same, 36 kilometers per second. The velocity for the cells of the target is zero. At the time, $t = 0$, the density is everywhere that of normal aluminum, 2.785 g per cm^3; the potential energy of compression, the pressure, and the pseudo-viscosity are all equal to zero.

The spatial velocity distribution, very soon after the impact starts, is shown by the solid line in Fig. 3. The presence of two shock fronts is apparent, one to the left into the thin plate and one to the right into the slab. Although the velocity of the shock front into the thin plate is opposite to the motion of the incident plate, the initial plate velocity is so great that this shock front is actually moving slowly to the right in the initial direction of the thin plate.

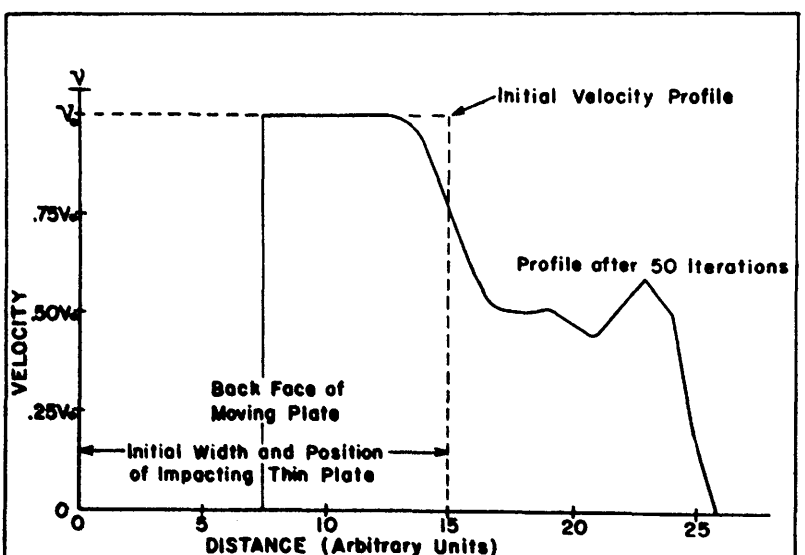

Figure 3. Velocity–Distance Profiles at Different Times.

Typical pressure profiles for different instants of time during the formation and propagation of the two shock fronts are presented in Figs. 4, 5, 6, 7 and 8. Each profile is labeled with N, the number of iterations which have been completed. Pressure-distance graphs are shown at intervals of approximately thirty iterations. The back edge of the thin plate is marked in each curve by a dashed line.

Soon after the impact starts, a single pressure peak starts at the interface between the thin plate and the slab. This is indicated in Fig. 4. The

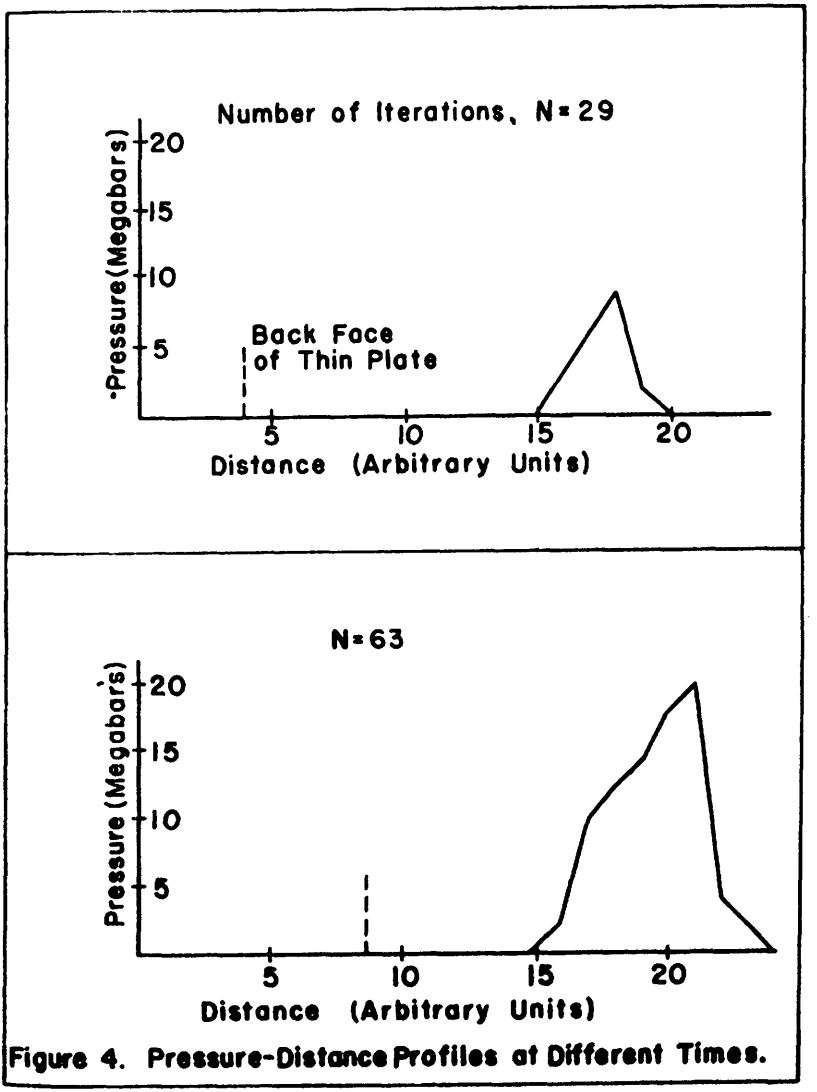

Figure 4. Pressure-Distance Profiles at Different Times.

growth and expansion of the pressure peak is shown in Fig. 5. The peak has grown but it is now predominantly in the face of the target slab.

As time progresses, two shock fronts of approximately equal strength develop as shown in Fig. 5. Although one front faces into the thin plate, it is really being carried to the right by the initial velocity of the thin plate. The other shock front is moving into the target at a rapid rate.

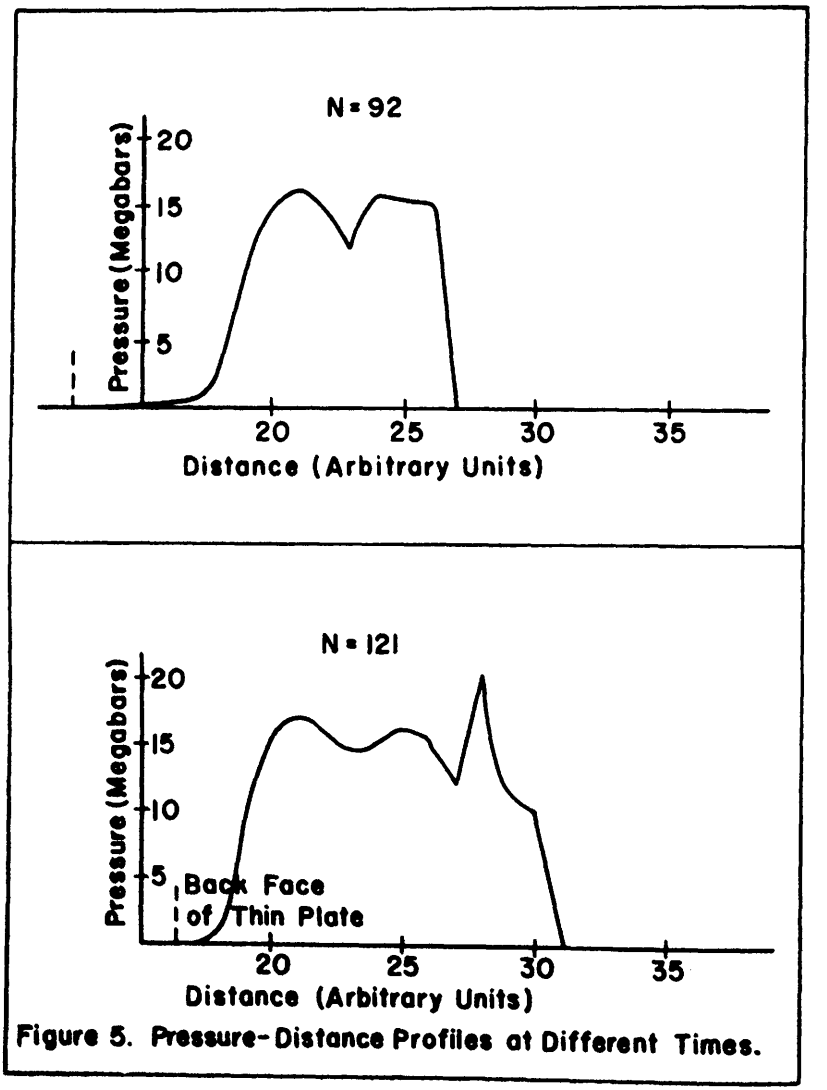

Figure 5. Pressure-Distance Profiles at Different Times.

A sharp decrease in pressure develops between the left and right shocks very early in the impact and is almost certainly real. It means that two shocks exist and they propagate substantially as separate shocks from soon after the initiation of the impact. The rarefaction wave from the back of the thin plate will effectively eliminate the shock into the thin plate and leave a single shock into the slab. A discussion of this phenomenon has been presented in a report (Todd, 1962).

The sharpness and exceptional height of the initial peak in these and other curves of the shock front is not real, but is a characteristic of the

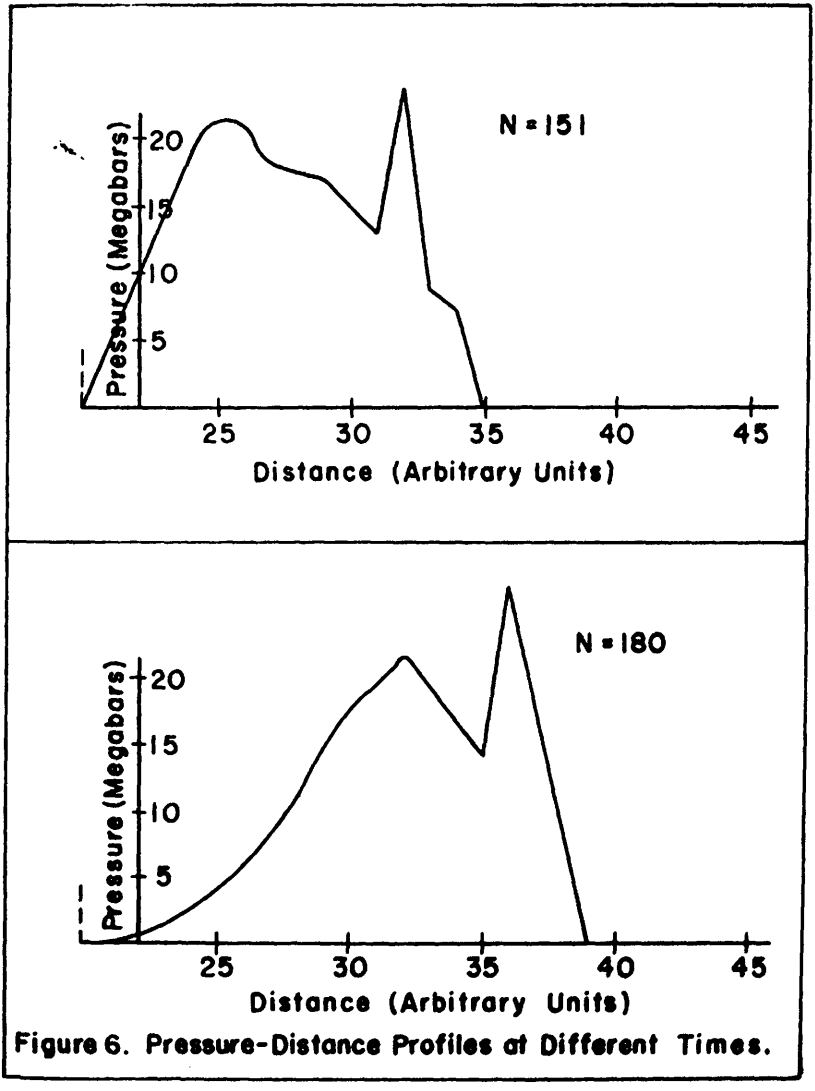

Figure 6. Pressure-Distance Profiles at Different Times.

computer and the size of the space interval. In the finite difference equations, the q-term tends to damp out this sharp peak, but in turn causes a dip immediately preceding the peak pressure.

The pressure distribution after 121 iterations is shown in the lower part of Fig. 5. The impact starts with the contact of the thin plate and the slab at 15. At the time for this curve, the back of the thin plate has penetrated completely past the initial position of the semi-infinite slab to about 16.5. The shock front into the thin plate has not yet reached the back face of this plate.

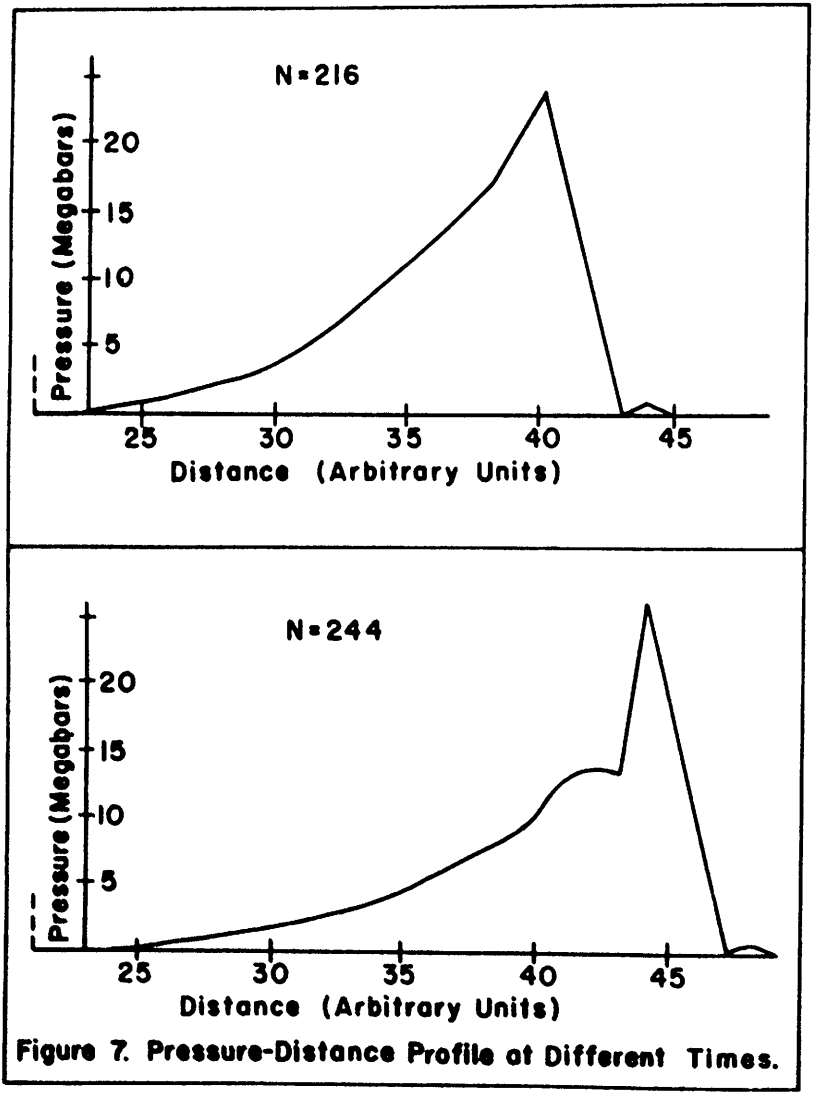

Figure 7. Pressure-Distance Profile at Different Times.

Profiles after 151 and 180 iterations are shown in Fig. 6. The thin plate continues to compress the material of the target and of itself. The penetration of the shock wave into the target material is now the important feature of the results. In the upper portion of the figure, the left traveling shock front has just reached the back face of the thin plate and will be reflected as a rarefaction wave. The development of this expansion with time is indicated in the lower part of the illustration. The back edge of the thin plate has practically come to a complete stop at a position of 20 units while the remaining shock wave now progresses into the aluminum with a peak pressure of about 20 megabars.

As time progresses, the shock from the impact becomes a single shock front propagating into the slab, as indicated in Fig. 7. The peak value of the shock pressure is probably false and is a result of employing large space intervals in the difference equations. The back edge of the plate remains stationary as the shock propagates into the slab. The shock front has reached a position of about 45 units after 244 iterations.

The last calculated profiles, in Fig. 8, indicate a decay in the strength of the shock front. Since the shock propagates into a non-viscous fluid, the decay results from two factors, the damping by the pseudo-viscosity and the spreading of the shock energy. The actual shock must propagate indefinitely into the slab until the increase in entropy at the shock front consumes all of the energy in the shock and this is a very slow process.

In summary, calculations were made and are presented which show the development of a traveling shock wave in a semi-infinite solid which is struck by a high-velocity thin plate. The hydrodynamic model also describes the existence of a second shock front moving from the point of contact into the thin plate and its reflection from the back edge of the thin plate as a decompression wave which travels into the semi-infinite slab.

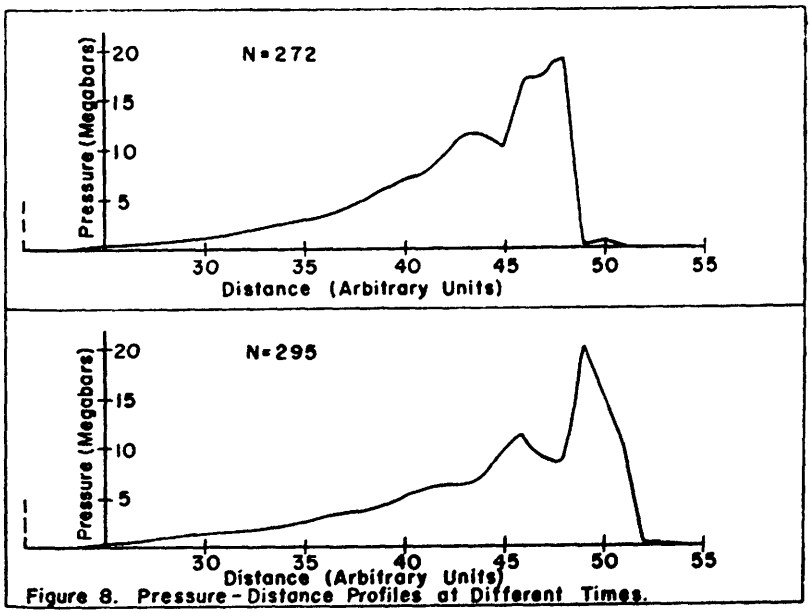

Figure 8. Pressure-Distance Profiles at Different Times.

LITERATURE CITED

Bjork, R. L. 1959. Effects of a micrometeoroid impact on steel and aluminum in space. Proc. Xth Internat. Astronautical Congress (London). Springer-Verlag, Vienna.

Lake, H. R., and F. C. Todd. 1962. Digital computer solution for the propogation of a spherical shock wave in aluminum. Proc. Okla. Acad. Sci. 42: 177-185.

Longley, H. J. 1960 (April). Los Alamos Scientific Laboratory, LAMS-2379.

Sodek, B. A., and F. C. Todd. 1963. Penetration of an initially radial shock wave through an aluminum-glass interface. Proc. Okla. Acad. Sci. 43: 173-82.

Todd, F. C., B. A. Sodek, L. Wang, and J. G. Ables. 1962 (July-Sept.). Quart. Progr. Rept. No. 8, Contract NASr-7. Oklahoma State University Research Foundation.

von Neumann, J., and R. D. Richtmyer. 1950. A method for the numerical calculation of hydrodynamic shocks. J. Appl. Phys. 21: 232-237.

Walsh, J. M., R. G. McQueen, and N. H. Rice. 1958. Compression of solids by strong shock waves. Solid State Physics, Advances in Research and Applications, 6: 1-63. Academic Press, New York.